Location of Mn in MnAPO-11: influence of synthesis from aqueous and non-aqueous media

A.K. Sinha, N.E. Jacob, D. Srinivas and S. Sivasanker *

National Chemical Laboratory, Pune 411 008, India
E-mail: siva@cata.ncl.res.in

MnAPO-11 samples were synthesized from aqueous (MnAPO-11(A)) and ethylene glycol (MnAPO-11(NA)) media. The crystallinity of the samples was more when the synthesis was carried out in ethylene glycol. Chemical and thermogravimetric analyses reveal greater incorporation of Mn in the framework of MnAPO-11(NA) than in MnAPO-11(A). At least five different types of Mn(II) species are detected in the samples by ESR. The studies suggest that Mn is more homogeneously distributed in MnAPO-11(NA) than in MnAPO-11(A).

Keywords: MnAPO-11 synthesis, Mn(II) ESR, MnAPO-11 ESR, aluminophosphate molecular sieves, manganese aluminophosphates

1. Introduction

Aluminophosphate ($AlPO_4$-n) molecular sieves are made up of a regular alteration of AlO_2^- and PO_2^+ tetrahedra and possess an overall neutral framework without ion-exchange capacity or strong acidity. They can be transformed into catalytically useful materials by introducing Brønsted acidity through the incorporation of lower valent metal (Me) ions in place of Al^{3+} (MeAPO; Me = Mg, Co, Mn, Zn, Fe, etc.) or by Si^{4+} in place of P^{5+} in the framework [1–6]. When Me^{2+} ions replace Al^{3+}, they are expected to be present in regular tetrahedral positions in the framework. However, a part of these ions can also be present in other locations such as defect sites, ion-exchange sites and extraframework positions. Besides, the distribution of the Me in the framework may be homogeneous or heterogeneous with "Me-rich" areas. From the angle of catalytic usefulness, the most desired locations are the isolated framework positions. The extent of incorporation, its location and distribution depend on the metal, the structural features of the $AlPO_4$ and preparation methods.

In the case of MnAPO-5, most of the Mn(II) ions were found to be in extraframework positions and inhomogeneously distributed even at low Mn contents [7]. On the other hand, Mn was incorporated mainly in framework positions in MnAPO-11 and MnAPSO-11 at low Mn contents, the extraframework component increasing with Mn content [8,9]. In MnAPSO-44, only 15% of the Mn was distributed homogeneously in the framework, the rest being situated in Mn-rich areas [10].

Earlier studies by us have revealed that the incorporation of Si^{4+} in SAPOs was dependent on the method of preparation of the samples [11,12]. For example, in the case of many structures, more Si was incorporated homo-

geneously as isolated species when the synthesis was carried out in ethylene glycol (non-aqueous medium) than in water [11,12]. In the present paper, we will examine the influence of the medium of synthesis (aqueous (A) or non-aqueous (NA)) on the location and distribution of Mn in MnAPO-11.

2. Experimental

MnAPO-11 samples A(0.05) and A(0.3) were hydrothermally synthesized from an aqueous medium following the method described by Messina et al. [2] and taking a gel composition of $1.0Al_2O_3 : xMnO : 1.0P_2O_5 : 1.0DPA : 50H_2O$ ($x = 0.05, 0.3$). Samples NA(0.1) and NA(0.3) were synthesized by making slight modifications in the above procedure, using ethylene glycol (EG) as the non-aqueous medium and taking a gel composition of $1.0Al_2O_3 : xMnO : 1.8P_2O_5 : 5.0DPA : 60EG$ ($x = 0.1, 0.3$). The values in parentheses denote the molar ratio of MnO in the initial gel. Aluminium isopropoxide (98%, Aldrich), orthophosphoric acid (85%, S.D. Fine-chem Ltd., India), dipropylamine (DPA, 99%, Aldrich) and $Mn(CH_3COO)_2 \cdot 4H_2O$ (99%, LOBA Chemie, India) were used in the syntheses.

In a typical synthesis from non-aqueous medium, aluminium isopropoxide (11.6 g) was added slowly to ethylene glycol (109.7 g) and the mixture was stirred for 1 h. Dipropylamine (14.2 g) was added dropwise to the mixture and further stirred for 1/2 h. Then, 11.5 g of orthophosphoric acid was added dropwise and stirred for another 1/2 h. Finally, 0.34 g of manganese(II) acetate (for 0.05 molar ratio) was added and the final mixture was stirred for 2 h more to get a homogeneous gel. This was transferred to a stainless-steel autoclave and heated at 473 K for 144 h.

---

* To whom correspondence should be addressed.

The synthesis products were washed with water, dried at 393 K for 6 h and calcined at 823 K for 8 h in air by gradually raising the temperature (2 K/min). One gram of the calcined sample was stirred in 100 ml of 1 M NaCl solution at 343 K for 5 h to exchange Na^+ for extraframework manganese.

The samples were characterized by X-ray powder diffraction (Rigaku model D/Max-VC, Cu K_α radiation, Ni filter, $\lambda = 1.5404$ Å), scanning electron microscopy (M/S Leica Cambridge Ltd., UK), and thermal analysis (Setaram, TG-DTA 92). Chemical composition was determined by atomic absorption spectroscopy (AAS for Al and Mn, Varian Spectr SF-220) and inductively coupled plasma with atomic emission spectroscopy (ICP-AES for P, Perkin–Elmer PE-1000). ESR experiments were performed on a Bruker EMX X-band ($\nu = 9.75$ GHz) spectrometer with a 100 kHz field modulation. Samples were taken in suprasil quartz tubes and the spectra were recorded at 298 and 77 K. Measurements at 77 K were done using a quartz insert Dewar. Spectral simulations and deconvolution were performed using Bruker WINEPR and Simfonia software packages.

3. Results and discussion

The XRD patterns of as-synthesized and calcined samples of MnAPO-11 prepared from both aqueous (A) and non-aqueous (NA) media were similar and crystallographic d values matched well with those reported earlier [2]. The crystallinity of the samples synthesized from the non-aqueous medium (NA) was higher than those from the aqueous medium (A). Chemical compositions of the calcined samples are listed in table 1. The analyses (table 1) revealed a lower Al content than P which is expected if Mn(II) replaces the Al sites within the framework.

Carbon and nitrogen analyses of the as-synthesized samples (table 1) indicate that the C/N ratios in the samples synthesized from aqueous and non-aqueous media are nearly the same, implying that ethylene glycol used in the synthesis (as non-aqueous medium) is not present inside the pores. Also the organic content of the non-aqueous samples is more than that of aqueous samples, indicating that more template is present inside the pores of the samples from non-aqueous medium than from the aqueous medium.

This is in agreement with the higher surface area for the former than the latter samples.

3.1. Thermogravimetric analysis

The TGA/DTA profiles of the as-synthesized samples A(0.3) and NA(0.3) are presented in figure 1. Four stages of weight loss at ∼363, ∼513, ∼753 and ∼873 K are observed in the thermograms of the samples carried out in flowing air. The first stage of weight loss is due to the desorption of physically adsorbed water. The other weight losses are probably due to the decomposition and combustion of the organic templating agent, dipropylamine. The
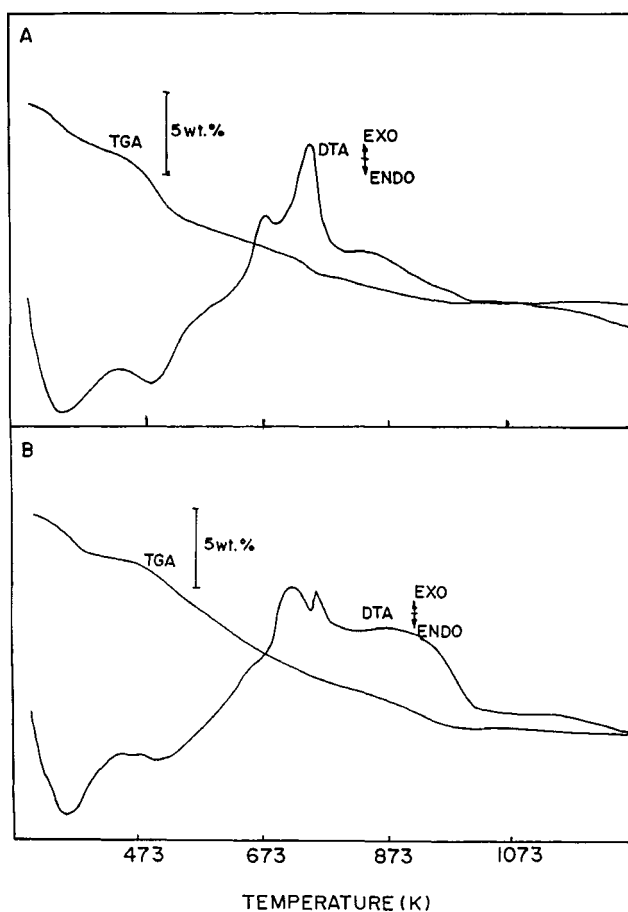

Figure 1. TGA/DTA profiles of as-synthesized MnAPO-11 samples. (A) MnAPO-11-A(0.3) and (B) MnAPO-11-NA(0.3).

Table 1
Physicochemical properties of MnAPO-11 samples.

Sample[a]	Composition[b]	Organics[c] (wt%)		S_{BET}[b] ($m^2 g^{-1}$)	TGA loss in stages[c] (wt%) (at temp. (K))			
		C	N		1	2	3	4
A(0.05)	$Al_{0.491}P_{0.507}Mn_{0.002}$	4.38	0.76	183	5.9 (382)	1.8 (513)	5.8 (644)	3.4 (818)
A(0.3)	$Al_{0.48}P_{0.48}Mn_{0.04}$	4.29	0.74	176	3.7 (363)	3.4 (503)	2.9 (743)	2.7 (853)
NA(0.1)	$Al_{0.44}P_{0.55}Mn_{0.01}$	5.94	1.01	222	3.5 (373)	3.3 (505)	4.4 (707)	2.8 (886)
NA(0.3)	$Al_{0.43}P_{0.54}Mn_{0.03}$	5.81	0.97	218	3.2 (371)	3.6 (513)	4.0 (766)	2.9 (895)

[a] Values in parentheses refer to molar ratio of Mn in the synthesis gel.

[b] Of calcined sample.

[c] In as-synthesized sample.

peak in the range 503–513 K is probably due to the physically adsorbed free dipropylamine and the subsequent peaks are due to the decomposition/combustion of the dipropylamine. The last two peaks are found to occur at higher temperatures for the non-aqueous (NA) samples compared to the aqueous (A) samples. This could be due to more Mn(II) substitution (for Al(III)) resulting in a larger charge buildup of the framework and stronger adsorption of the organic molecules in the non-aqueous samples (NA).

3.2. Scanning electron microscopy

Figure 2 shows the SEM photographs of two MnAPO-11 samples. While the crystals of A(0.3) are composed of microcrystallites aggregated into irregular shaped (cauliflower like) particles, the crystals of NA(0.3) are well defined spheroids. The SEM pictures confirm the XRD observations of the samples NA being more crystalline than the samples A.
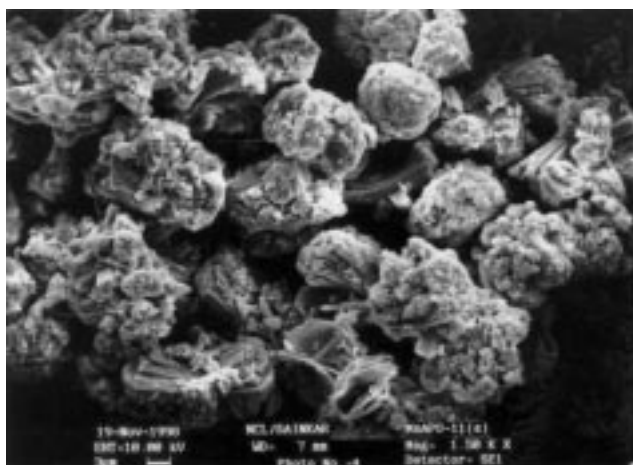
(a)
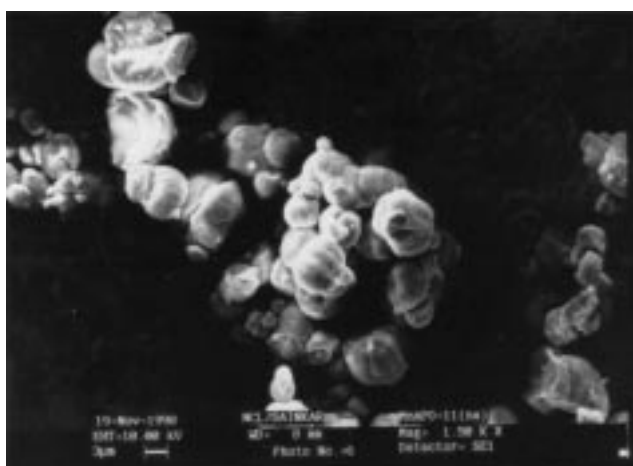
(b)

Figure 2. Scanning electron micrographs of (a) MnAPO-11-A(0.3) and (b) MnAPO-11-NA(0.3).

3.3. ESR studies

When Mn(II) is incorporated in $AlPO_4$ molecular sieves, its possible locations are as follows:

(i) isolated Mn(II) in regular or defect (broken) framework Al sites,

(ii) isolated extraframework Mn(II) in exchange locations,

(iii) patches containing two or more Mn(II) ions occupying the nearby or adjacent Al positions, and

(iv) small clusters of bulk MnO in the extraframework locations.

In fact, Mn(II) ions are present in all these locations in our samples, though the proportions of the various species depend on the method of preparation (aqueous or non-aqueous) and the amount of Mn(II) incorporated.

The ESR spectrum of Mn(II) ion in an octahedral or tetrahedral environment ($3d^5 : t_{2g}^3 e_g^2$ electronic configuration) can be described by the following generalized spin Hamiltonian [13]:

$$\mathcal{H} = g\beta SB_0 + A_{Mn}IS + D\left[S_z^2 - 35/12\right]$$
$$+ E\left(S_x^2 - S_y^2\right) + (1/6)a\left[S_x^4 + S_y^4 + S_z^4 - 707/16\right]$$
$$+ (1/180)F\left[35S_z^4 - (475/2)S_z^2 + (3255/16)\right],$$

where β is the Bohr magneton, D and E are axial and rhombic zero-field parameters which are sensitive to the distortions and site geometry, a and F are cubic field parameters and A_{Mn} is the hyperfine coupling constant due to interaction of the nuclear spin and electron spins ($I = 5/2$, $S = 5/2$) of manganese. For a perfect octahedral or tetrahedral geometry, D and E are equal to zero. But for a lower symmetry, these zero-field terms are non-vanishing and the spectrum consists of five sets of six hyperfine features corresponding to $m_s = |+5/2\rangle \leftrightarrow |+3/2\rangle$, $|+3/2\rangle \leftrightarrow |+1/2\rangle$, $|+1/2\rangle \leftrightarrow |-1/2\rangle$, $|-1/2\rangle \leftrightarrow |-3/2\rangle$ and $|-3/2\rangle \leftrightarrow |-5/2\rangle$ fine structure transitions. However, in a disordered (powder or polycrystalline) state the spectrum mainly consists of the central six lines due to the $m_s = |+1/2\rangle \leftrightarrow |-1/2\rangle$ transition, while the signals for $|\pm5/2\rangle \leftrightarrow |\pm3/2\rangle$ and $|\pm3/2\rangle \leftrightarrow |\pm1/2\rangle$ transitions are usually not resolved due to the presence of more than one magnetically inequivalent Mn(II) site with different zero-field distortion parameters (D and E) and contribute only to the background upon which the central sextet pattern ($m_s = |+1/2\rangle \leftrightarrow |-1/2\rangle$) is superimposed [15,16]. Manganese being an S-state ion, the sextet pattern centers around the free spin g value (2.0023). ESR spectra for the samples under consideration are sensitive to the method of preparation, Mn content and treatment conditions. Experiments were performed on three Mn concentrations (molar ratios of 0.05, 0.1 and 0.3) to derive meaningful information about the site locations of Mn(II) in MnAPO-11 samples prepared from aqueous (A) or non-aqueous (NA) media.

As-synthesized samples of MnAPO-11(A and NA) at 298 K showed spectra consisting of six hyperfine features
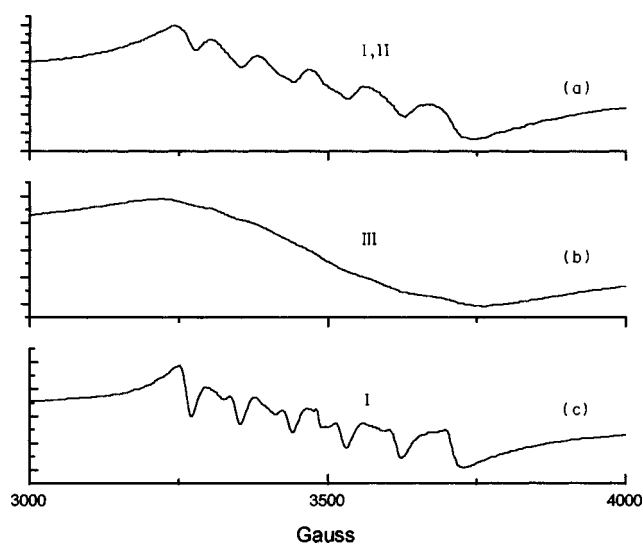
Figure 3. X-band ESR spectra of MnAPO-11-A(0.05) at 298 K. (a) As-synthesized, (b) calcined, and (c) Na$^+$-exchanged sample. Corresponding signals due to species I and II (isolated octahedral Mn(II) in framework and exchange positions) and species III (spin–spin coupled Mn(II)) are indicated.

Figure 4. X-band ESR spectra of MnAPO-11-A(0.3) at 298 K. (a) As-synthesized, (b) calcined, (c) Na$^+$-exchanged and dried at 473 K, and (d) after rehydration of (c). Signals due to species IV (distorted framework sites) and species V (bulk MnO$_x$) are indicated.

Figure 5. X-band ESR spectra of MnAPO-11-NA(0.3) at 298 K. (a) As-synthesized, (b) calcined, (c) Na$^+$-exchanged and calcined at 473 K, and (d) rehydrated samples of (c). Signals due to isolated substituted sites (d) are more clearly seen for samples prepared from non-aqueous than from aqueous medium.

centred at $g = 2.0039$. The separation between the adjacent hyperfine features is unequal, as shown in figure 3(a), for A(0.05) and increases from 72 to 112 G, while the linewidth (ΔH_{pp}) changes from 37.5 to 75.5 G in the direction of increasing field. The average manganese hyperfine coupling constant (A_{Mn}) and linewidth (ΔH_{pp}) were estimated to be 92 and 59 G, respectively. These hyperfine features are well resolved for samples with lower Mn content. Moreover, the spectra in second-derivative mode indicated additional splitting on each hyperfine feature probably due to the presence of more than one type of isolated Mn(II) centers (say, e.g., framework-substituted and exchange locations) with different crystal field environments. The g and A_{Mn} values match very well with those reported by Kevan et al. [8,9] for framework-substituted MnAPO-11. The value of 92 G for A_{Mn} corresponds to octahedral coordination for Mn(II). It is to be noted that octahedral coordination of Al locations in many AlPO$_4$s including AlPO$_4$-11 [18] is known. Although the value of A_{Mn} falls in the range of values reported for isolated Mn(II) species, the peak-to-peak linewidth is larger than that reported for octahedral Mn(II) in extraframework positions of MnMCM-41 [19] and zeolites X and Y [20]. Measurements at 77 K did not provide any additional information. At higher Mn content the hyperfine features are relatively less resolved (figures 4 and 5). Spectral simulations reveal the presence of two types of signals, a broad signal with a peak-to-peak linewidth of about 500 G over which the major central sextet pattern is superimposed. The intensity of the broad signal is more for the high Mn content samples (A/NA(0.3)) than for the low Mn content samples (A(0.05) and NA(0.1)). While the signals with a sextet pattern are attributed to isolated Mn(II) centres in framework (species I) and exchange positions (species II), the broad signal is assigned to Mn(II) ions in
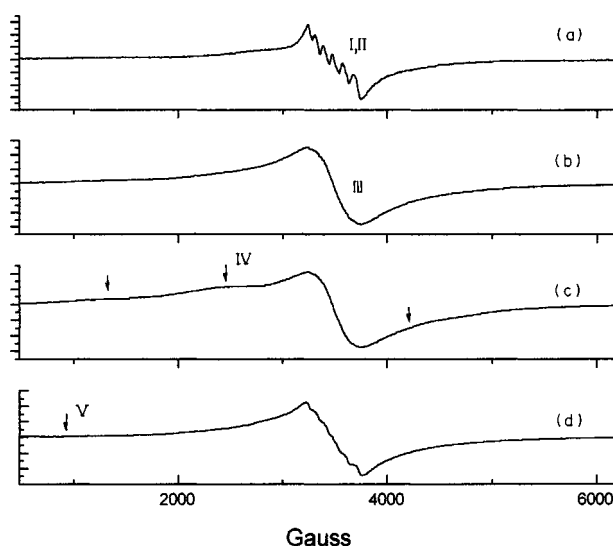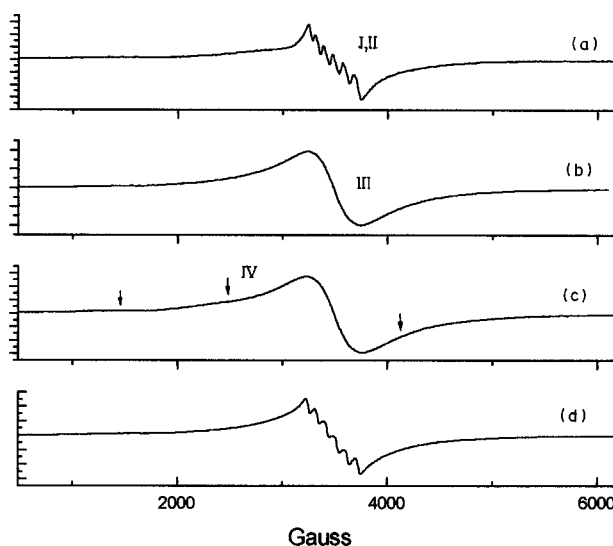
adjacent framework locations forming patches (species III) and exhibiting nearest neighbour spin–spin interactions.

Calcined samples of MnAPO(A) and MnAPO(NA) show, in contrast, a major broad signal ($\Delta H_{pp} = 500$ G for sample A and 550 G for sample NA) at $g = 2.004$ and weak signals at 1650 G ($g_{eff} = 4.27$) and 2850 G ($g_{eff} = 2.42$). Weak signals (sextet) attributable to isolated Mn(II) locations are also seen, but these became broader upon calcination ($\Delta H_{pp} = 84.5$ G) and submerged by the major broad signal (figures 3(b), 4(b) and 5(b)). Similar broad signals have also been observed for Mn-containing MCM-41 [19], MnAPO-5 [7] and MnAPSO-44 [10]. The origin

Table 2
EPR parameters and assignments for different Mn(II) species.

Species	g	ΔH_{Mn}[a] (G)	A_{Mn}[a] (G)	Assignment and location
I, II	2.0039	59 (60)	92 (95)	Octahedral framework (I)/exchange sites (II)
III	2.004	500 (550)	–	Interacting Mn(II) ions as patches in framework
IV	4.27, 2.42, 1.47	–	–	Distorted tetrahedral framework sites
V	∼15	–	–	Interacting MnO_x type extraframework sites

[a] Values in parentheses are for non-aqueous samples.

of the broad signal could be as follows. On calcination the water of hydration and template molecules are lost and Mn(II) ions in exchange positions come closer to each other and to the framework ions. This migration of paramagnetic centres towards the framework results in extraframework–framework Mn(II) interactions and, hence, a broad ESR signal. In other words, the dominating broad signal in calcined samples corresponds to both Mn(II) framework patches (species III) as well as interacting extraframework–framework Mn(II) centers. The signals at 1650 and 2850 G are due to zero-field splitting contributions (D and $E \neq 0$) for some isolated Mn(II) sites in distorted framework locations (species IV) [19,21,22]. The normalized overall signal intensity obtained by double integration of the ESR spectrum is more (four times for sample A and nine times for sample NA) for calcined than for as-synthesized samples. This could be because of the differences in the nature of the paramagnetic species in calcined and as-synthesized samples. In the latter, the major species are the isolated Mn(II) centres exhibiting narrower signals, while in the former they are the interacting Mn(II) species showing broad signals.

Upon Na^+ ion exchange, sample A(0.05) shows a well resolved hyperfine sextet pattern with average A_{Mn} being 89.7 G. Forbidden transitions ($\Delta M_I = \pm 1$) are also visible in between the six allowed ($\Delta M_I = 0$) transitions (figure 3(c)). The enhanced resolution of the spectra could be due to the removal of the extraframework Mn(II) (by Na^+) which had broadened the signals through Mn(II)–Mn(II) interactions. The sextet pattern observed for Na^+-exchanged samples may be attributed mainly to framework substituted manganese (species I). No major difference in the spectra was observed for samples with high Mn content (figures 4(c) and 5(c)). The broad signal corresponding to species III and moderately intense signals at $g_{eff} = 4.22$, 2.68 and 1.47 corresponding to species IV are the main features of these spectra. The signals due to species IV, though weakly observed in calcined samples, became more prominent after Na^+ exchange and drying.

Upon exposure to water vapour (ambient atmosphere, relative humidity ∼80%), the samples exhibit a resolved six-line pattern corresponding to species I with an average line width of 64 G and A_{Mn} of 96 G (figures 4(d) and 5(d)). The six-line pattern is more intense and better resolved in MnAPO-11(NA) than in MnAPO-11(A) probably due to a more homogeneous distribution of the isolated Mn(II) sites (species I) in the former sample. Sample A(0.3) shows an additional broad signal at $g \approx 15$, which cannot be attributed to monomeric Mn(II) ion but can be associated with the exchange-coupled Mn(II) oxide clusters in extraframework positions (figure 4(d)). This signal disappeared upon dehydration at 423 K for 16 h. This low field signal was not observed for samples prepared from non-aqueous medium. ESR parameters and assignments of different Mn species in MnAPO-11(A and NA) are listed in table 2.

The above studies suggest that the distribution of Mn is more homogeneous in samples synthesized from ethylene glycol, with a larger proportion of isolated Mn(II) species than in the samples synthesized from aqueous medium. Bulk MnO type species was present in MnAPO-11(A) samples having high Mn content. This was notably absent in the MnAPO-11(NA) samples. The ESR studies confirm the observations made based on the composition and TGA/DTA studies of the sample that Mn(II) incorporation in the framework is more in MnAPO-11(NA) than in MnAPO-11(A).

4. Conclusions

MnAPO-11 samples with three Mn contents were synthesized from aqueous and non-aqueous media and characterized. MnAPO-11 samples prepared from ethylene glycol (non-aqueous medium) result in more crystalline material than those by conventional procedures in an aqueous medium. Thermogravimetric studies suggest that more Mn is incorporated in the framework when synthesized from ethylene glycol. X-band ESR spectra reveal that Mn(II) in MnAPO-11 is present as five types of species, viz. isolated framework and extraframework sites with octahedral co-ordination and reversible hydration/dehydration behaviour, small patches containing two or three nearby framework Mn(II) ions, isolated framework sites with distorted geometry and bulk manganese oxide species. The Mn ions are more homogeneously distributed in the samples prepared from ethylene glycol (with a larger proportion of Mn in isolated framework sites) than those from aqueous medium.

References

[1] S.T. Wilson and E.M. Flanigen, US Patent 4567029 (1986).
[2] C.A. Messina, B.M. Lok and E.M. Flanigen, US Patent 4544143 (1985).
[3] C.J. Wright and N.B. Milestone, Eur. Patent Appl. 0141662 (1985).
[4] D.R. Pyke, P. Whitney and H. Houghton, Appl. Catal. 18 (1985) 173.

[5] G.C. Bond, M.R. Gelsthrope and K.S. Sing, J. Chem. Soc. Chem. Commun. (1985) 1056.

[6] E.M. Flanigen, B.M. Lok, R.L. Patton and S.T. Wilson, Pure Appl. Chem. 58 (1986) 1351.

[7] Z. Levi, A.M. Raitsimring and D. Goldfarb, J. Phys. Chem. 95 (1991) 7830.

[8] C.W. Lee, X. Chen, G. Brouet and L. Kevan, J. Phys. Chem. 96 (1992) 3110.

[9] G. Brouet, X. Chen, C.W. Lee and L. Kevan, J. Am. Chem. Soc. 114 (1992) 3720.

[10] Z. Olender (Levi), D. Goldfarb and J. Batista, J. Am. Chem. Soc. 115 (1993) 1106.

[11] N. Venkatathri, S.G. Hegde, P.R. Rajmohanan and S. Sivasanker, J. Chem. Soc. Faraday Trans. 93 (1997) 3411.

[12] A.K. Sinha, S. Sivasanker and P. Ratnasamy, Ind. Eng. Chem. Res. 37 (1998) 2208.

[13] A. Abragam and B. Bleary, in: *Electron Paramagnetic Resonance of Transition Ions* (Clarendon, Oxford, 1970) ch. 7, p. 378.

[14] J.E. Wertz and J.E. Bolton, *Electron Spin Resonance, Elementary Theory and Practical Applications* (McGraw-Hill, New York, 1977) ch. 10, p. 223.

[15] T.I. Barry and L.A. Lay, J. Phys. Chem. Solids 27 (1966) 1821.

[16] T.I. Barry and L.A. Lay, Nature 208 (1965) 1312.

[17] H.A. Kuska and M.T. Rogers, in: *Radical Ions* (Wiley/Interscience, New York, 1968) p. 579.

[18] M. Goepper, F. Guth, L. Delmotte, J.L. Guth and H. Kessler, Stud. Surf. Sci. Catal. 49 (1989) 857.

[19] J. Xu, Z. Luan, T. Wasowicz and L. Kevan, Micropor. Mesopor. Mater. 22 (1998) 179.

[20] N.N. Tikhomirova and I.V. Nikolaeva, Russ. J. Phys. Chem. 55 (1981) 2224.

[21] P.P. Knops-Gerrits, M. Labbe and P.A. Jacobs, Stud. Surf. Sci. Catal. 108 (1997) 445.

[22] D.L. Griscom and R.E. Griscom, J. Chem. Phys. 47 (1967) 2711.